Journal of the Optical Society of America A
OPTICS, IMAGE SCIENCE, AND VISION

An analytical model of the influence of cone sensitivity and numerosity on the Rayleigh match

LI ZHAOPING[1,*] AND JOSEPH CARROLL[2]

[1]University College London, London, UK
[2]Medical College of Wisconsin, Milwaukee, Wisconsin 53226, USA
*Corresponding author: z.li@ucl.ac.uk

Received 28 September 2015; revised 13 January 2016; accepted 16 January 2016; posted 19 January 2016 (Doc. ID 250942); published 19 February 2016

The Rayleigh match is defined by the range of mixtures of red and green lights that appear the same as an intensity-adjustable monochromatic yellow light. The perceptual match indicates that the red–green mixture and the yellow light have evoked the same respective cone absorptions in the L- and M-cone pathways. Going beyond the existing models, the Poisson noise in cone absorptions is proposed to make the matching proportion of red–green mixtures span a finite range because any mixture in that range evokes cone absorptions that do not differ from those by a yellow light by more than the variations in the absorption noise. We derive a mathematical formula linking the match midpoint or match range with the sensitivities and numerosities of the two cones. The noise-free, exact, matching point, close to the midpoint of the matching range, depends only on the L- and M-cone sensitivities to each of the red, green, and yellow lights [these sensitivities, in turn, depend on the preferred wavelengths (λ_{max}) and optical densities of the cone pigments and the properties of prereceptoral light filtering]. Meanwhile, the matching range depends on both these cone sensitivities and the relative numerosity of the L and M cones. The model predicts that, in normal trichromats, all other things being equal, the match range is smallest when the ratio r between L and M cone densities is $r = R^{-1/2}$ with R as the ratio between the sensitivities of the L and M cones to the yellow light, i.e., when L and M cones are similarly abundant in typical cases, and, as r departs from $R^{-1/2}$, the match range increases. For example, when one cone type is 10 times more numerous, the match range increases two- to threefold, depending on the sensitivities of the cones. Testing these model predictions requires either a large data set to identify the effect of one factor (e.g., cone numerosity) while averaging out the effects of the other factors (e.g., cone sensitivities) or for all factors to be known. A corollary of this prediction is that, because they are more likely than usual to have L:M cone ratios skewed, the matching ranges of normal female trichromats who are carriers of dichromacy (but not anomalous trichromacy) are likely to have a larger matching range than usual, particularly for the deutan carriers. In addition, the model predicts that, in strong tetrachromats (whose four dimensions of color are preserved post-receptorally), either the Rayleigh matching is impossible or the matching range is typically smaller than usual.

OCIS codes: (330.0330) Vision, color, and visual optics; (330.1690) Color; (330.5310) Vision - photoreceptors.

http://dx.doi.org/10.1364/JOSAA.33.00A228

1. INTRODUCTION

The Rayleigh match [1] is a procedure to classify color vision, e.g., to diagnose color-blindness or color vision abnormality. In this procedure, a test subject views a circular field of about 2° in diameter split into top and bottom halves. The upper hemifield contains a mixture of red and green monochromatic lights (with wavelengths $\lambda_R \approx 670$ and $\lambda_G \approx 545$ nm, respectively) of given intensities R and G, respectively, and the lower hemifield contains a yellow monochromatic light (of wavelength $\lambda_Y \approx 589$ nm). The red–green mixture is adjusted by having a fraction f of the red light combined with a fraction $(1 - f)$ of the green light, and the intensity Y of the yellow light is also adjusted, such that, at some values of f and Y, the two hemifields are matched in appearance; see Fig. 1. The range of f, and its midpoint, to achieve the match are used to classify color vision. Although readouts of typical anomaloscopes, e.g., the Nagel anomaloscope [2], in practice scale the f values to the range between 0 and 70, this paper uses the range $0 \le f \le 1$ by the definition of fraction.

Normally, humans have three types of cones, sensitive to short (S), medium (M), and long (L) wavelengths of light, with their sensitivities peaking at the wavelength $\lambda_{max} \approx 420$, 530,

and 557 nm, respectively [3]. Hence, the S cones are not appreciably excited by any of the three lights (R, G, Y) in the Rayleigh matching procedure, which thus only classifies color vision characters involving the properties of the L and M cones. Normal trichromats, who have normal L and M cones, typically have a small matching range near $f = 0.5$ (given a suitable calibration of the light intensities R and G and their wavelengths) [4]. Dichromats lacking L cones (protanopia) or M cones (deuteranopia) can match with any f values. Observers with defective L (protanomaly) or M (deuteranomaly) cones are called anomalous trichromats. As $\lambda_{\max}$ of the defective L/M cones are shifted toward the $\lambda_{\max}$ of the normal M/L cones, anomalous trichromats typically have a relatively large matching f range with a midpoint f away from the typical f values for the normals.

It has long been recognized that the Rayleigh match is achieved when the two hemifields are identical in terms of their excitations evoked in the normal or abnormal L and/or M cones of the observer. Accordingly, models of the Rayleigh match have been developed [5–8]. Given the input light from each hemifield, the cone excitations from this hemifield can be calculated from the (wavelength) spectral sensitivity curves of the cones; these curves, in turn, depend on the following cone and retinal properties: $\lambda_{\max}$ of the cone pigments, the optical densities of the cone pigments, and the light filtering properties of the optical medium in the retina before input light reaches the cones. These models help us to examine how changes in cone and retinal properties, such as $\lambda_{\max}$ and the optical densities of the cone pigments, affect the matching value f. In this paper, we present an analytical model aimed to gain additional insights that are not easily achieved using the numerical methods employed by the previous models. Furthermore, we propose that the nonzero matching range of f is caused by the noise in the cone excitations—zero noise would give a zero matching range and an exact matching point f (except in dichromats)—and derive a formula for the matching range, which, to the best of our knowledge, has not been previously modelled. In particular, we show that, while the exact matching point f depends only on the spectral sensitivities of the cones (given the light properties), the matching range is also influenced by the relative densities of the L and M cones on the retina. In addition, we present specific and experimentally testable predictions from this model with some discussions.

2. AN ANALYTICAL MODEL OF THE RAYLEIGH MATCH

The relevant properties of the retinal cones and the anomaloscope are as follows: (1) the pair of fixed intensities R and G for the red and green light, respectively, and the adjustable intensity Y of the yellow light; (2) three pairs of sensitivities of the L and M cones, respectively, to the three lights: r_L and r_M to the red light, g_L and g_M to the green light, and y_L and y_M to the yellow light; and (3) the pair of fractions, n_L and n_M (such that $n_L + n_M = 1$), of the cones that are L and M, respectively. We will show, analytically and intuitively using graphics, how these five pairs of values (each in a bracket),

$$(R, G), (r_L, r_M), (g_L, g_M), (y_L, y_M), (n_L, n_M), \quad (1)$$

determine the Rayleigh match and the matching range.

Given the sensitivities r_L and r_M of the L and M cones to the red light, the cone responses to the red light of intensity R are Rr_L and Rr_M, represented as a point $R(r_L, r_M)$ (a row vector with components Rr_L and Rr_M) in the 2D space of the cone responses in Fig. 2(A). Similarly, cone responses to the green light are represented by the point $G(g_L, g_M)$ in Fig. 2(A). The line connecting these two points contains points representing the cone responses to the red–green mixtures. Let L_{RG} and M_{RG} denote the L cone and M cone's responses to a red–green mixture; then, to a mixture with a fraction $0 \le f \le 1$ of the red light,

$$(L_{\mathrm{RG}}, M_{\mathrm{RG}}) = f \cdot R(r_L, r_M) + (1 - f) \cdot G(g_L, g_M). \quad (2)$$

A f closer to $f = 1$ gives a point $(L_{\mathrm{RG}}, M_{\mathrm{RG}})$ closer to $R(r_L, r_M)$ on that red–green mixture line in Fig. 2(A).

Meanwhile, the cone responses to the yellow lights are

$$(L_Y, M_Y) = Y(y_L, y_M), \quad (3)$$

the points $Y(y_L, y_M)$ with various $Y \ge 0$ make another line originating from the origin in Fig. 2(A). The Rayleigh matching is defined by

$$(L_{\mathrm{RG}}, M_{\mathrm{RG}}) = (L_Y, M_Y), \quad (4)$$

when the two lines in Fig. 2(A) intersect each other. Let α be the angle between the yellow line and horizontal; then, a point on this yellow line with a distance y from origin can be written as

$$(L_Y, M_Y) \equiv (y \cos(\alpha), y \sin(\alpha)). \quad (5)$$

Figure 2(B) shows that any point $(L_{\mathrm{RG}}, M_{\mathrm{RG}})$ on the red–green mixture line can be decomposed to two components: one along the yellow-light line, with a distance A from the origin, and another perpendicular to it with a deviation D to the yellow-light line. Hence, the angle between deviation D and horizontal axis is $\pi/2 + \alpha$, making the unit vector along D as $(-\sin(\alpha), \cos(\alpha))$. Therefore, quantity D is the dot product of vector $(L_{\mathrm{RG}}, M_{\mathrm{RG}})$ with this unit vector:

$$D = (L_{\mathrm{RG}}, M_{\mathrm{RG}}) \cdot (-\sin(\alpha), \cos(\alpha)), \quad (6)$$

i.e., D is the projection of $(L_{\mathrm{RG}}, M_{\mathrm{RG}})$ on $(-\sin(\alpha), \cos(\alpha))$. The Rayleigh match happens when $D = 0$. Using Eq. (2) and noting

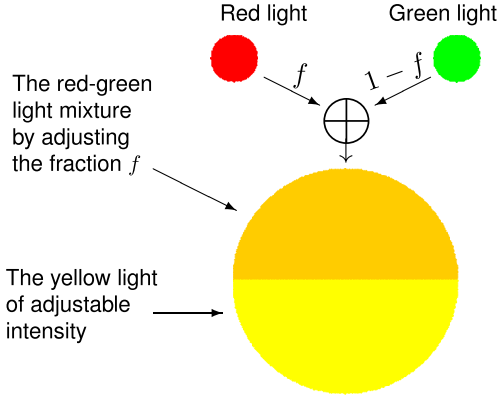

Fig. 1. Rayleigh match is achieved when the mixture made of a fraction f of the red light and a fraction $1 - f$ of the green light appears identical to the yellow light with a suitable intensity.

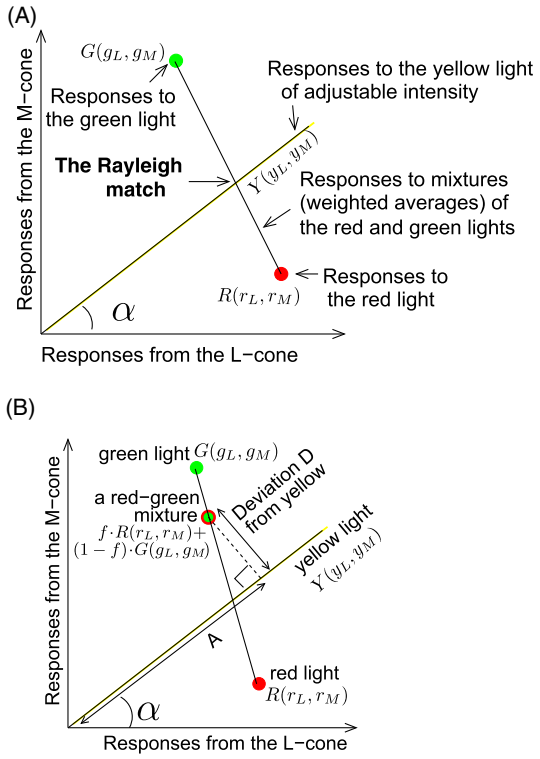

Fig. 2. (A) Phase space of L and M cone activations to various lights: red, green, yellow, and red–green mixtures. The Rayleigh match is made when the cone activations to the yellow light are the same as that to a red–green mixture. The yellow line forms an angle α with the horizontal axis. (B) Cone activation to any red–green mixture can be decomposed to two components: A, the component along the yellow light activations, and D, deviation from the yellow light activations. When $D = 0$, the Rayleigh match is achieved. In the text, the responses to the yellow light are (L_Y, M_Y); the responses to the red–green mixture light are (L_{RG}, M_{RG}).

$$\cos(\alpha) = y_L/(y_L^2 + y_M^2)^{1/2}, \qquad \sin(\alpha) = y_M/(y_L^2 + y_M^2)^{1/2}, \tag{7}$$

we have

$$D = \frac{1}{(y_L^2 + y_M^2)^{1/2}}[Q_2 - f(Q_1 + Q_2)], \text{ in which} \tag{8}$$

$$Q_1 \equiv R(r_L y_M - r_M y_L), \qquad Q_2 \equiv G(g_M y_L - g_L y_M). \tag{9}$$

and analogously Q_3, Q_4, Q_5, and Q_6, introduced later, are quantities built from our five pairs of values in Eq. (1). The Rayleigh matching is to adjust the fraction f to make $D = 0$ and adjust the yellow light intensity to make $y = A$. Solving $D = 0$ for the matching f value gives

$$f_{\text{match}} = \frac{1}{1 + (Q_1/Q_2)}. \tag{10}$$

Therefore, given the red and green light intensities R and G, and the three pairs of L and M cone sensitivities (r_L, r_M), (g_L, g_M), and (y_L, y_M) to the three lights, the matching fraction f_{match} is determined by the above formula.

The three pairs of cone sensitivities can be read out from the spectrum sensitivity curves $S_L(\lambda)$ and $S_M(\lambda)$, respectively, of the L and M cones, as the sensitivity values $S_{L,M}(\lambda)$ for the wavelengths $\lambda = \lambda_R$, λ_G, and λ_Y of the three monochromatic light sources; see Fig. 3. (For general, nonmonochromatic lights, the three pairs of sensitivities are, e.g., $r_L = \int d\lambda S_L(\lambda) I_i(\lambda)$ for the input spectrum $I_i(\lambda)$, with $\int d\lambda I_i(\lambda) = 1$, of the light source $i = R, G, Y$.) The sensitivity spectrum $S_{L,M}(\lambda)$, in turn, depend on the $\lambda_{\max}$ and optic density $O_{L,M}$ of the photopigment for the cone and the optical density spectra $O_{\text{lens}}(\lambda)$ of the retina lens and $O_{\text{macular}}(\lambda)$ of the macular layer as follows. For cone $C = L$ or M,

$$S_C(\lambda) = (1 - 10^{-O_C \cdot E(\lambda, \lambda_{\max})}) 10^{-O_{\text{lens}}(\lambda) - O_{\text{macular}}(\lambda)}, \tag{11}$$

$$\text{with} \quad E(\lambda, \lambda_{\max}) = (e^{E_1} + e^{E_2} + e^{E_3} + 0.655)^{-1},$$

$$E_1 = 70\left(0.88 - \frac{\lambda_{\max}}{\lambda}\right),$$

$$E_2 = 28.5\left(0.924 - \frac{\lambda_{\max}}{\lambda}\right),$$

$$E_3 = -14.1\left(1.104 - \frac{\lambda_{\max}}{\lambda}\right),$$

where O_C is the optical density of the photopigment and $E(\lambda, \lambda_{\max})$ is called the extinction coefficient of the cone [9]. In typical human eyes, $O_{\text{lens}}(\lambda)$ and $O_{\text{macular}}(\lambda)$ are negligible at the wavelengths of our concern. Hence, a cone's sensitivity curve is largely determined by its $\lambda_{\max}$ and optical density O_C of the pigment. As summarized in Fig. 4, variations of $\lambda_{\max}$ (caused by genes, even among normal trichromats) and O_C lead to variations in the three pairs of cone sensitivities (r_L, r_M), (g_L, g_M), and (y_L, y_M), which, in turn [by Eq. (10)], cause

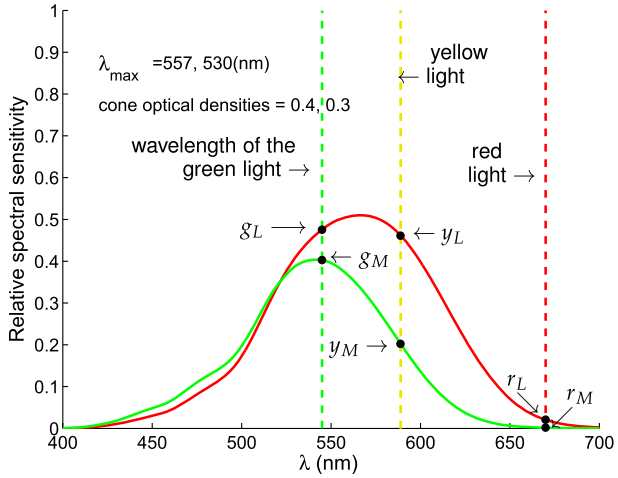

Fig. 3. Spectral sensitivities $S_L(\lambda)$ and $S_M(\lambda)$ of the L and M cones by Eq. (11), and illustrations of the three pairs of sensitivities (r_L, r_M), (g_L, g_M), and (y_L, y_M) to the three lights. Different $\lambda_{\max}$ and optical densities of the cones can alter these six numbers. These six numbers (and the intensities R and G of the red and green light) determine the matching point f_{match}, but the matching range depends in addition on the L:M cone ratio.

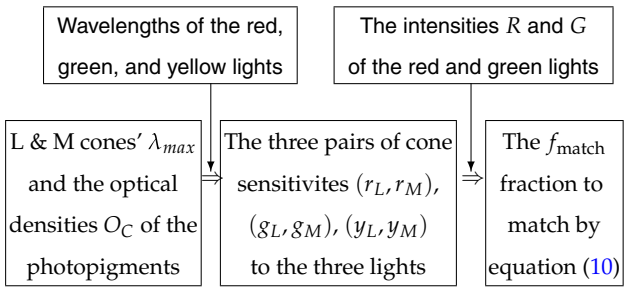

Fig. 4. Summary of how retinal and cone properties determine the outcome of the Rayleigh match.

variations in the Rayleigh match f_{match} between different observers.

Let us define our standard trichromat as one with the following λ_{max} and optical density O_C (slightly different from the example in Fig. 3) of the pigment for the cones and the pre-receptor properties:

$$\begin{aligned} &\text{L cone } \lambda_{\text{max}} = 557(\text{nm}), \qquad O_L = 0.4, \\ &\text{M cone } \lambda_{\text{max}} = 530(\text{nm}), \qquad O_M = 0.4, \\ &\text{Pre-receptor}: \; O_{\text{lens}}(\lambda) \quad \text{and} \quad O_{\text{macular}}(\lambda) \text{ are as in [10].} \end{aligned} \tag{12}$$

Let us also define our standard anomaloscope as the one with

$$\begin{aligned} &\text{The three primaries with } \lambda_R, \lambda_G, \lambda_Y = 670, 545, 589 \text{ nm.} \\ &\text{The light intensities } R \text{ and } G \text{ give } R/G \approx 23.4 \text{ and } G = 1. \end{aligned} \tag{13}$$

We note from Eqs. (9) and (10) that f_{match} depends only on the ratio R/G and not R and G individually. Hence, given R/G, we can arbitrarily set $G = 1$, as we did above, without affecting f_{match} (although the yellow-light intensity needed for the matching scales with G). This R/G ratio above is for the "deutan mode" of the anomaloscope calibration [6], so that the red and green lights excite the L cone equally (i.e., $Rr_L = Gg_L$) for our standard trichromat defined above. Our standard trichromat should thus obtain $f_{\text{match}} \approx 0.5$ using our standard anomaloscope.

A. Any Fraction f Achieves a Match for Dichromats

One way to view dichromats lacking the L or M cone is to consider their L and M cones as identical to each other. For example, consider protanopia as when the L cones are just copies of the M cones. Hence, these dichromats have $r_L = r_M$, $g_L = g_M$, $y_L = y_M$, and, from Eq. (7), $\cos(\alpha) = \sin(\alpha)$. Hence, $Q_1 = Q_2 = 0$ by Eq. (9), and, consequently, any fraction f gives $D = 0$ by Eq. (8) to achieve the match. Graphically, $r_L = r_M$, $g_L = g_M$, and $y_L = y_M$ together means that, in Fig. 2(A), the line for the red–green mixtures and that for the yellow lights are both on the diagonal line from the origin (45° from horizontal), so that all the red–green mixture points are on the line for the yellow lights.

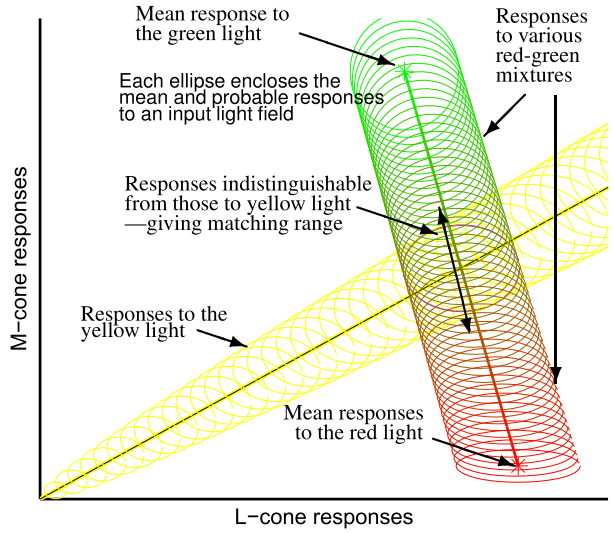

Fig. 5. Illustration of how noise in cone responses lead to a finite, nonzero, range of matching fractions. Each ellipse schematically illustrates the range of probable cone responses that could be evoked by an input light whose average evoked cone responses is marked by the center of the ellipse. The yellow ellipses enclose probable responses to the yellow light; red, green, and red–green ellipses enclose probable responses to the red, green, and mixture lights. The horizontal and vertical extents, respectively, of each ellipse visualize the standard deviations of the noises in L and M cones. When two input light fields give substantially overlapping response ellipses, these two inputs match perceptually, i.e., not perceptually distinguishable. Hence, a finite range of red–green mixtures can match the yellow light fields.

B. Protanomaly Requires More Red Light to Match

The light intensities R and G are calibrated such that quantities in Eq. (10) for normal trichromats give $Q_1 \sim Q_2$, making $f_{\text{match}} = 1/(1 + Q_1/Q_2) \sim 0.5$. In protanomaly, the λ_{max} of the L cones is abnormally reduced toward the λ_{max} of the (normal) M cones, altering r_L, g_L, and y_L, accordingly. Because (see Fig. 3) the r_L value is very near the tail of L cone's spectral sensitivity curve, while g_L and y_L are near the peak of this curve, a reduction in λ_{max} for the L cones reduces r_L by a large percentage while leaving g_L and y_L relatively unchanged in percentage. Consequently, $Q_1 = R(r_L y_M - r_M y_L)$ is much reduced while $Q_2 = G(g_M y_L - g_L y_M)$ is relatively unchanged, making f_{match} larger to require more red light for the match as observed in observers with protanomaly. Figures 6(A) and 6(B) illustrate how a protanomalous differs from normal in the match.

C. Deuteranomaly Requires More Green Light to Match

In deuteranomaly, the λ_{max} of the M cones is abnormally increased toward the λ_{max} of the (normal) L cones. Among the affected sensitivities r_M, g_M, and y_M, only the g_M value sits near the peak of the cone sensitivity spectrum. As a result, percentage-wise, r_M and y_M are both much increased while g_M is relatively unchanged. Consequently, $Q_2 = G(g_M y_L - g_L y_M)$ is much reduced, whereas $Q_1 = R(r_L y_M - r_M y_L)$ is less likely to change by as much in percentage, leading to a reduced f_{match}

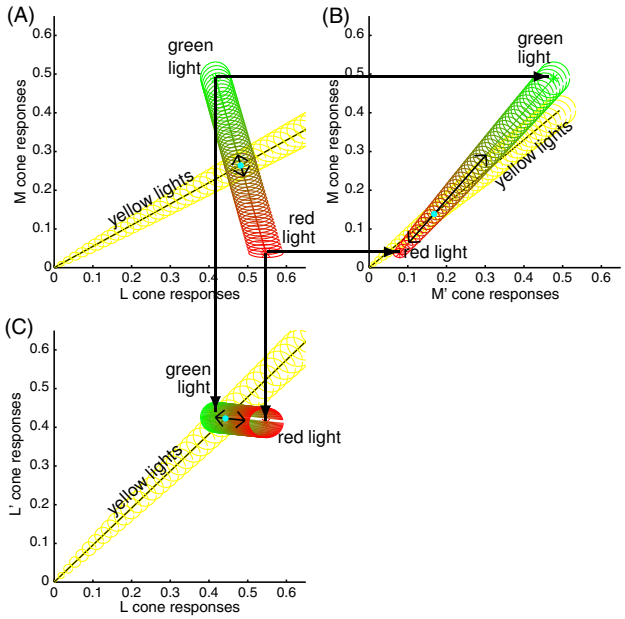

Fig. 6. Comparing matching in a normal trichromat (A), a protanomalous (B), and a deuteranomalous (C). The two horizontal black arrows from (A) panel to (B) panel indicate that the M cone responses in protanomalous are copies of those in normal trichromats. Similarly, the two vertical black arrows from (A) panel to (C) panel indicate that the L cone responses in deuteranomalous are copies of those in normal trichromats. The abnormal cone is the M′ cone in panel (B) and L′ cone in panel (C). In protanomalous (B) and deuteranomalous (C), the two cone types have similar responses for any typical input (when the two cone pigments have the same optical density). For protanomalous (B), this makes the line for the yellow light and the line for the red–green mixtures nearly parallel or identical to each other. For deuteranomalous (C), this makes cone responses insensitive to changes in the fraction f of the red–green mixture (because intensities of red and green lights in typical anomaloscope are calibrated to evoke similar L cone responses). In each panel, the cyan dot marks the matching point, and the black double arrow spans the matching range schematically; the length of the black arrow as a fraction of the total distance between the mean responses to the red and green lights is the numerical matching range (e.g., in both (B) and (C), $f_{\text{matching-range}} \sim 0.5$).

to require more green light for the match as observed in observers with deuteranomaly. Figures 6(A) and 6(C) illustrate how a deuteranomalous differs from normal in the match.

D. Matching Range from Cone Absorption Noise

Cone absorptions are noisy. Each input, whether a red–green mixture or a yellow light, can evoke many possible pairs of L and M cone responses randomly distributed around the mean response pair. Consequently (see Fig. 5), responses to the mixtures and yellow lights are no longer confined to, but distributed around, the two lines of zero thickness in the 2D L-M response space. This is as if the lines become thicker by the typical magnitudes of the cone response noise. The noise blurs small differences between two input fields so that a red–green mixture could appear identical to a yellow light even if the mixing fraction f deviates a little from f_{match}. Hence, a range of f values around f_{match} can produce mixtures to match the yellow light.

Consider a red–green mixture with a $f = f_{\text{match}} + \Delta f$. Let the zero-noise L-M cone responses to this mixture deviate by a displacement D from the zero-noise responses to the yellow light [see Fig. 2(B)]. Cone noise makes D also a noisy variable, with an average $\overline{D}$ given by Eq. (8) and a standard deviation σ_D determined by the noises in the L and M responses. When $|\overline{D}| \le \sigma_D$, i.e., the average D is within the range of the noise blurs, the red–green mixture should appear indistinguishable from the nearest yellow light.

Using Eq. (8) and noting that $\overline{D} = 0$ for $f = f_{\text{match}}$ by definition, we have $\overline{D} \propto \Delta f$ as

$$\overline{D} = \frac{1}{(y_L^2 + y_m^2)^{1/2}} (\Delta f)(Q_1 + Q_2). \tag{14}$$

The largest two $|\Delta f|$'s, one for a negative Δf_1 and one for a positive Δf_2, to make $\overline{D}^2 = \sigma_D^2$ should make the matching range in $f \in (f_{\text{match}} + \Delta f_1, f_{\text{match}} + \Delta f_2)$, making the matching range:

$$f_{\text{matching-range}} \equiv \Delta f_2 - \Delta f_1. \tag{15}$$

Noise in cone absorption is Poisson like [11], so that the variances $\sigma^2(L_{\text{RG}})$ and $\sigma^2(M_{\text{RG}})$ of noise in L and M cone responses, respectively, scale with the respective average responses, L_{RG} and M_{RG}:

$$\sigma^2(L_{\text{RG}}) = L_{\text{RG}}, \qquad \sigma^2(M_{\text{RG}}) = M_{\text{RG}} \tag{16}$$

(more accurately, noise variance scales with average response by a Fano factor larger than unity [11], but this discrepancy will be absorbed by our parameter β introduced later). In addition, noise in the L and M cones are independent of each other. Therefore, because D is a weighted sum of L and M cone responses [with weights $-\sin(\alpha)$ and $\cos(\alpha)$; see Eq. (8)], the variance σ_D^2 in D is also a weighted sum (with weights $\sin^2(\alpha)$ and $\cos^2(\alpha)$) of the respective variances in the L and M responses:

$$\sigma_D^2 = \sigma^2(L_{\text{RG}})\sin^2(\alpha) + \sigma^2(M_{\text{RG}})\cos^2(\alpha), \tag{17}$$

$$= L_{\text{RG}} \sin^2(\alpha) + M_{\text{RG}} \cos^2(\alpha). \tag{18}$$

Using Eqs. (2) and (7), and $f = f_{\text{match}} + \Delta f$, we have

$$\sigma_D^2 = \frac{1}{y_L^2 + y_m^2}\{(\Delta f + f_{\text{match}})(Q_3 - Q_4) + Q_4\}, \text{ in which}$$

$$Q_3 \equiv R(r_L y_M^2 + r_M y_L^2), \qquad Q_4 \equiv G(g_L y_M^2 + g_M y_L^2). \tag{19}$$

From Eq. (14), $|\overline{D}|^2 = \sigma_D^2$ gives (noting that $f_{\text{match}} = 1/(1 + Q_1/Q_2)$)

$$(\Delta f)^2(Q_1 + Q_2)^2 + (Q_4 - Q_3)\Delta f - \frac{Q_2 Q_3 + Q_1 Q_4}{Q_1 + Q_2} = 0. \tag{20}$$

Because the quantities Q_1, Q_2, Q_3, and Q_4 are built from four pairs of values, (R, G), (r_L, r_M), (g_L, g_M), and (y_L, y_M), the two solutions Δf_1 and Δf_2 to give the matching range [by Eq. (15)] are determined by these four pairs of values.

Thus far, we have ignored the fact that many L and M cones on the retina receive visual input from the light fields. While the number of cones does not matter for f_{match}, it does for Δf because pooling responses from many cones can smooth out the noise. Let there be N_L L cones and N_M M cones

responding to each light field, define $N \equiv N_L + N_M$ and $n_L \equiv N_L/N$ and $n_M \equiv N_M/N$. Pooling the cones means to multiply sensitivities (r_L, g_L, y_L) by Nn_L and (r_M, g_M, y_M) by Nn_M in calculating $\overline{D^2}$ and σ_D^2. In addition, define Q_i for each $i = 1, 2, 3, 4$ as the Q_i when each r_L, g_L, or y_L is replaced by $n_L r_L$, $n_L g_L$, or $n_L y_L$, respectively, and each r_M, g_M, or y_M is replaced by $n_M r_M$, $n_M g_M$, or $n_M y_M$, respectively. Then, Eq. (20) becomes

$$N(\Delta f)^2(\hat{Q}_1 + \hat{Q}_2)^2 + (\hat{Q}_4 - \hat{Q}_3)\Delta f - \frac{\hat{Q}_2\hat{Q}_3 + \hat{Q}_1\hat{Q}_4}{\hat{Q}_1 + \hat{Q}_2} = 0. \tag{21}$$

Then, an $N \to \infty$ requires $\Delta f \to 0$, because the signal-to-noise diverges when responses are pooled over infinitely many cones. However, our central brain does not seem to be able to integrate signals over infinitely many cones or over an infinitely long viewing duration to smooth out noise [12–14]; otherwise, all signal-to-noise in the central decision stage will approach infinity to give infinite accuracy to color matching and other similar sensory-matching tasks. This limit in our central brain is implemented here by replacing an $N \to \infty$ by a noninfinite parameter β. Hence, replacing N by β in the above equation and solving for Δf from it,

$$\Delta f = \frac{\hat{Q}_3 - \hat{Q}_4 \pm \sqrt{(\hat{Q}_3 - \hat{Q}_4)^2 + 4\beta(\hat{Q}_1 + \hat{Q}_2)(\hat{Q}_2\hat{Q}_3 + \hat{Q}_1\hat{Q}_4)}}{2\beta(\hat{Q}_1 + \hat{Q}_2)^2}. \tag{22}$$

Hence, by Eq. (15),

$$f_{\text{matching-range}} = \frac{\sqrt{(\hat{Q}_3 - \hat{Q}_4)^2 + 4\beta(\hat{Q}_1 + \hat{Q}_2)(\hat{Q}_2\hat{Q}_3 + \hat{Q}_1\hat{Q}_4)}}{\beta(\hat{Q}_1 + \hat{Q}_2)^2}, \tag{23}$$

which can be approximated for normal trichromats [because their $(\hat{Q}_3 - \hat{Q}_4)^2$ is relatively negligible] by

$$f_{\text{matching-range}} \approx 2\left(\frac{\hat{Q}_2\hat{Q}_3 + \hat{Q}_1\hat{Q}_4}{\beta(\hat{Q}_1 + \hat{Q}_2)^3}\right)^{1/2} \tag{24}$$

$$= \frac{2}{\sqrt{\beta}}\left(\frac{Q_5}{(Q_1 + Q_2)^3}\right)^{1/2}\left(\frac{y_L}{n_M} + \frac{y_M}{n_L}\right)^{1/2} \tag{25}$$

$$\text{in which } Q_5 \equiv GRy_L y_M(r_L g_M - r_M g_L). \tag{26}$$

Let us extend the definition of our standard trichromat in Eq. (12) to have relative L and M cone densities such that $n_L = 2/3$ (so that $n_M = 1/3$), and let this trichromat have $f_{\text{matching-range}} = 0.04$ using our standard anomaloscope in Eq. (13). Then, $\beta \approx 13135$ is required for this $f_{\text{matching-range}}$. We can use this numerical β value in Eq. (25) or (23) for $f_{\text{matching-range}}$ of general observers with normal or abnormal color vision, if we assume that this central limiting parameter β is the same across different observers.

E. Variable Matching Ranges for Anomalous Trichromats

By Eq. (23), the matching range $f_{\text{matching-range}}$ increases when the denominator $\beta(\hat{Q}_1 + \hat{Q}_2)^2$ in the right-hand side of this equation decreases. Because $\hat{Q}_1 \propto r_L y_M - r_M y_L$ and $\hat{Q}_2 \propto g_M y_L - g_L y_M$ [see Eq. (9)], we have $\hat{Q}_1 \approx 0$ and $\hat{Q}_2 \approx 0$ when $r_L \approx r_M$, $g_L \approx g_M$, and $y_L \approx y_M$, i.e., when the L and M cones are very similar. Hence, $\hat{Q}_1 + \hat{Q}_2$, and thus the denominator, approaches zero in anomalous trichromats, whose L and M cones have similar λ_{max} (assuming that the two cone types have the same optical density). Therefore, these observers are likely to have larger matching ranges than normal.

This qualitative conclusion still holds when the L and M cones have different optical densities, O_L and O_M, for the photopigments. This is because, approximately, the effect of optical densities [see Eq. (11)] merely scales the L cone sensitivities r_L, g_L, and y_L by one factor associated with O_L and scales the M sensitivities r_M, g_M, y_M by another factor associated with O_M. Hence, even when $r_L \approx r_M$, $g_M \approx g_L$, and $y_L \approx y_M$ no longer hold, $r_L y_M \approx r_M y_L$ and $g_M y_L \approx g_L y_M$ still hold to make $\hat{Q}_1 \approx 0$ and $\hat{Q}_2 \approx 0$.

Figure 6 shows a graphical understanding of the above conclusion. For protanomalous or deuteranomalous, the ratio L cone response : M cone response is nearly a constant across input variations, because L and M cones have similar λ_{max} (this constant is one when L and M pigments have the same optical density). For protanomalous [Fig. 6(B)], this makes the line for red–green mixtures and the line for the yellow lights nearly parallel or identical to each other, making more mixtures indistinguishable from the yellow lights. For deuteranomalous [Fig. 6(C)], this makes the cone responses nearly invariant to the fraction changes in the red–green mixture. In particular, when the anomaloscope is calibrated at or around the deutan mode, defined as when the red and green lights equally excite a standard L cone, the similarity in spectral sensitivity of the two cone mechanisms in deuteranomalous individuals (L and L′) means that the response of neither the L nor the L′ cone varies substantially with the fraction changes in the red–green mixture. Hence, more compositions of the red–green mixture can appear identical to the matched yellow lights when noise blurs small response differences.

Large matching ranges in anomalous trichromats have been observed experimentally [15]. However, the matching behavior of color deficient observers is highly variable so that some have small matching ranges [16–18]. This could be understood by noting that a smaller denominator $\beta(\hat{Q}_1 + \hat{Q}_2)^2$ in the formula for $f_{\text{matching-range}}$ in Eq. (23) makes the value of $f_{\text{matching-range}}$ more sensitive to variations in the value of the numerator in this formula. In particular, when the numerator is too small, a small $f_{\text{matching-range}}$ results, even though, in general, a smaller denominator yields a larger $f_{\text{matching-range}}$. Pinpointing $f_{\text{matching-range}}$ for an individual requires knowing both the sensitivities and relative numerosities of the L and M cones present in a given retina. In any case, because the denominator is smaller for anomalous trichromats than that for the normals, $f_{\text{matching-range}}$ is not only more likely larger, but also more highly variable, among anomalous trichromats.

F. Match Range Increases for Normal Trichromats When the Numbers of L and M Cones Differ by Too Much

Because $f_{\text{matching-range}}$ also depends on the relative cone densities n_L and n_M [see Eq. (25) or (23)], normal trichromats can also have larger $f_{\text{matching-range}}$ for some n_L/n_M. To study the effect of n_L/n_M in normal trichromat, we use the approximation of $f_{\text{matching-range}}$ by Eq. (25), rewritten here:

$$f_{\text{matching-range}} \approx \frac{2}{\sqrt{\beta}}\left(\frac{Q_5}{(Q_1+Q_2)^3}\right)^{1/2}\left(\frac{y_L}{n_M}+\frac{y_M}{n_L}\right)^{1/2}, \tag{27}$$

which isolates the dependence of $f_{\text{matching-range}}$ on n_L/n_M in the factor (note that $n_L + n_M = 1$):

$$Q_6 \equiv \left(\frac{y_L}{n_M}+\frac{y_M}{n_L}\right)^{1/2} = \left(\frac{y_L}{1-n_L}+\frac{y_M}{n_L}\right)^{1/2}, \tag{28}$$

the other $(\ldots)^{1/2}$ factor in $f_{\text{matching-range}}$ depends only on the light intensities (R and G) and the three pairs of cone sensitivities (r_L, r_M), (g_L, g_M), (y_L, y_M). Solving $dQ_6/dn_L = 0$ gives, with all other things being equal,

$$f_{\text{matching-range}} \text{ is minimum when } n_L = \frac{\sqrt{y_M}}{\sqrt{y_L}+\sqrt{y_M}} \tag{29}$$

(see Fig. 7). A tenfold change in n_L/n_M from a typical $n_L/n_M \approx 1$ can increase $f_{\text{matching-range}}$ by twofold or more, more so when y_L/y_M deviates more from unity. Figure 7(A) illustrates the Rayleigh matching in four example values of n_L/n_M when (r_L, r_M), (g_L, g_M), (y_L, y_M) are fixed. Intuitively, because the ratio (total L cone response) : (total M cone response) scales with n_L/n_M, each point in Fig. 7(A) is scaled along the horizontal and vertical axes by the corresponding n_L and n_M, respectively. Consequently, the line for the red–green mixtures and the line for the yellow lights become increasingly more parallel to each other when n_L/n_M deviates more from unity; this, in turn, increases the overlap between the two noise-thickened lines near their intersection to make $f_{\text{matching-range}}$ larger.

The impact of n_L/n_M on $f_{\text{matching-range}}$ (particularly in normal trichromats) is a prediction that can be tested. However, $f_{\text{matching-range}}$ also changes with the cone sensitivities [(r_L, r_M), (g_L, g_M), and (y_L, y_M)], which also determine f_{match}. Holding f_{match} fixed does not nail down $f_{\text{matching-range}}$ because there are four underlying variables (λ_{max} and O_c for each of the L and M cone types) to determine the cone sensitivities (assuming the anomaloscope and the pre-receptor retinal filters are fixed). Once $n_L = n_M = 0.5$ is fixed, collective variations of each λ_{max} within the range of 3–4 nm and each O_C within a factor of 2–3 can cause $f_{\text{matching-range}}$ to vary within a range of about twofold. Therefore, testing the predicted effect of cone numerosity on $f_{\text{matching-range}}$ should require either a large number of observers to average out the variations caused by the variations of cone sensitivities or a group of observers whose cone sensitivities (or related specifics) are precisely known.

G. Matching Difficulties and Smaller Matching Ranges for Strong Tetrachromats

Human tetrachromats are observers who have four functioning types of cones. We consider those tetrachromats who have three functioning types of cones, which are, unlike the S cones, sensitive to the wavelengths of the red, green, and yellow lights for the Rayleigh match. For example, a heterozygous female carrier of anomalous trichromacy can possibly be a tetrachromat by having a normal L cone, a normal M cone, and an abnormal L or abnormal M cone [19]. We consider the case of strong tetrachromats when post-receptor processing preserves the extra dimension of color information by the additional cone type (as opposed to weak tetrachromats when the extra color dimension is lost post-receptorally) [20]. For these individuals, a match requires that each of the three (rather than two) types of cones is activated equally by the two light fields: one red–green

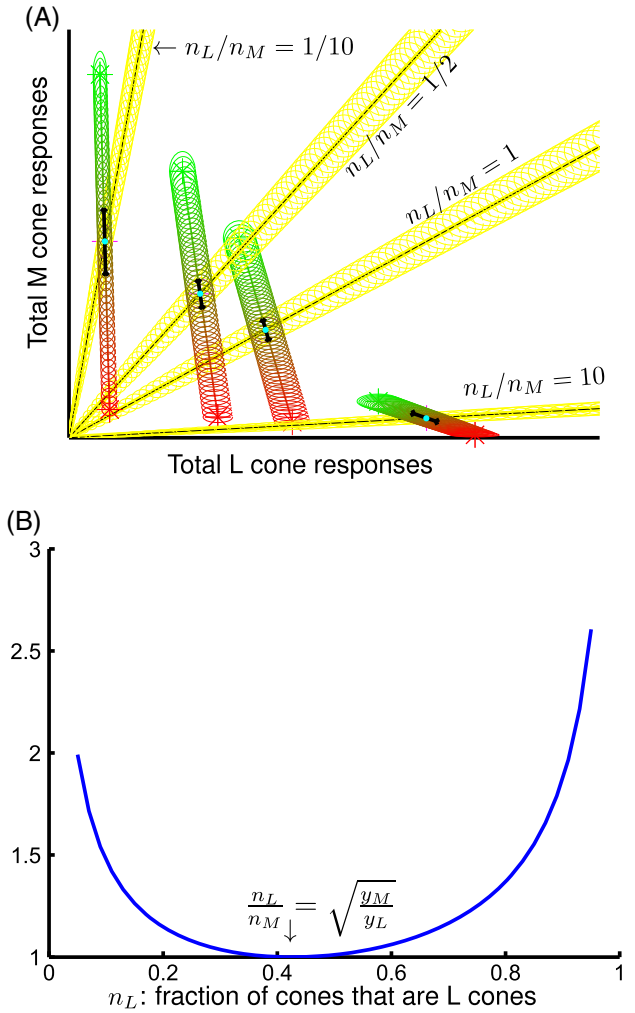

Fig. 7. Effects of the relative L versus M cone numerosities on the matching range $f_{\text{matching-range}}$. (A) Schematic illustrations of four examples of normal trichromats with the same three pairs of sensitivities (r_L, r_M), (g_L, g_M), and (y_L, y_M), but different relative L and M cone numerosities. The black double arrows schematically spans the matching range; the cyan dots mark the f_{match} locations. (B) The $f_{\text{matching-range}}$ relative to its minimum value (which occurs at $n_L = \frac{\sqrt{y_M}}{\sqrt{y_L}+\sqrt{y_M}}$) versus $n_L (= 0.05\text{–}0.95)$, showing that, all other things being equal, $f_{\text{matchin-grange}}$ increases when L cones are too many or too few relatively. $y_L/y_M = 1.82$ in both (A) and (B).

mixture and one yellow light. When there is no noise in cone activations, such a match is not mathematically possible because it would require satisfying simultaneously three equations, one for each cone type, by only adjusting two variables, the mixing fraction f and the yellow-light intensity. Graphically, this impossibility can be understood by generalizing Fig. 2(A) from a 2D space to a 3D space, with the three axes representing the respective responses from the three cone types. In this 3D space, two lines of the cone responses, one for the red–green mixture and one for the yellow light, are unlikely to intersect each other for the exact match. In practice, when cone activation noise is considered, however, a match may still be possible for such a tetrachromat if the closest distance or gap between the two lines is within the noise range—the f value and the yellow light intensity to achieve this closest distance is then the matching point, and the noise amplitude is sufficient to bridge the gap. If the noise is not sufficient to bridge the gap, such a tetrachromat would not be able to find a match.

For tetrachromats who can achieve a match, the matching range is likely smaller than usual because the above-mentioned gap makes it more difficult for any fraction f to achieve a match even with the cone noise. This smaller matching range can also be understood using the example when the relevant three cone types consist of the normal L cone, the normal M cone, and an abnormal L cone. A match involving these three cone types is equivalent to two simultaneous two-cone matches, one involving only the normal L cone and the normal M cone, another involving only the abnormal L cone and the normal M cone. The matching range for the three-cone match should be the intersection between two matching ranges for the two respective two-cone matches and, therefore, should be smaller than usual. For example, if the matching range for the Rayleigh matching involving the normal L and M cones is $f_1 \in (0.48, 0.51)$ and that for a match involving the abnormal L and the normal M cones is $f_2 \in (0.50, 0.60)$, then the matching range involving all the three cones is $f \in (0.50, 0.51)$. If the first two matching ranges do not overlap, then the tetrachromat will not find any fraction f to achieve a satisfactory match.

3. SUMMARY AND DISCUSSION

We introduce an analytical model of the Rayleigh match, so that the matching fraction f_{match} is expressed by an explicit mathematical formula [in Eq. (10)], showing how f_{match} depends on the three L-M pairs of cone sensitivities [(r_L, r_M), (g_L, g_M), and (y_L, y_M)] to the three lights (the sensitivities in turn are precisely determined by the λ_{max} and optical densities of photopigments, properties of the pre-receptor retinal filter, and the wavelengths [or spectrum compositions] of the three lights for the anomaloscope) and on the intensities R and G of the red and green lights. In addition, we propose that the noise in the cone responses are responsible for the nonzero matching range and used the Poisson nature of the noise in the cones to derive another mathematical formula for the matching range [in Eq. (23) or, as an approximation for normal trichromats, Eq. (25)]. The matching range is shown to be influenced not only by the same retinal and anomaloscope quantities [(r_L, r_M), (g_L, g_M), (y_L, y_M), R, and G] that determined the matching fraction f_{match} but also by the relative numbers n_L and n_M of L and M cones.

We also introduced a graphical understanding of the Rayleigh match, as shown, for example, in Figs. 2 and 5–7. Together, the graphical understanding and the analytical formulae enabled us to understand why dichromats can match in any red–green mixtures, why protanomalous needs more red light and deuteranomalous needs more green light for the match, why cone absorption noise makes the matching range nonzero, why anomalous trichromats have larger matching ranges than the normal trichromats, and how relative L and M cone numerosities influence the matching range.

In addition, our model and understanding provide the following four predictions, which can be tested by experimental data.

1. Everything else being equal, matching range in normal trichromats is larger when L and M cones have very different relative numerosities. For example, when there are 10 times as many cones of one type as that of the other type, the matching range $f_{\text{matchin-grange}}$ can be about two or three times as large as that when the two types of cones have comparable numerosities.
2. Female normal trichromats who are also carriers of dichromacy (i.e., they have one X chromosome with genes for the normal cones and another X chromosome lacking the gene for the L or M cone) are more likely to have larger matching ranges than noncarrier normal trichromats.
3. On average, the matching range in the female deutan carriers is larger than that in the female protan carriers.
4. The matching range in strong tetrachromats is typically smaller than that in the typical normal trichromats, and that the Rayleigh matching is impossible in some strong tetrachromats.

Next, we elaborate on and discuss these predictions.

For prediction 1, because, given numerosities of the cones, the $f_{\text{matching-range}}$ can also vary by two- to threefold due to variations in λ_{max} and optical densities of the photopigments among the normal trichromats, the predicted effects by the numerosities of the cones are best tested among observers having the same sensitivities of the cones. Alternatively, we can also employ many observers so that variabilities of $f_{\text{matching-range}}$ caused by the variabilities of the cone sensitivities can be averaged out among the observers. We note that, due to variabilities in both the numerosities and sensitivities of the cones among normal trichromats, $f_{\text{matching-range}}$ can vary by up to about tenfold. A previous work [8] had speculated that this roughly tenfold change may be caused by the same roughly tenfold change in the relative numerosities of the L and M cones among the normal trichromats [21,22]. Our analytical modeling, however, enables us to predict that a tenfold change in the relative numerosities only causes about two- to threefold change in the $f_{\text{matching-range}}$.

Prediction 2 is a corollary of prediction 1 because female normal trichromats who are also carriers of dichromacy are more likely to have extreme n_L/n_M values. Ignoring the S cones for simplicity, if each photoreceptor randomly expresses one of the L and M genes from only one of the X chromosomes [23], the retina is more likely to have fewer cones of the type whose gene is lacking in the dichromacy X chromosome. In particular,

we can calculate the modified fraction n'_L of the L cones in these carriers using a simple model as follows. Assume that (1) only one X chromosome is activated to express a cone for each photoreceptor, and let p be the chance that this X chromosome is the normal one; and (2), if the normal X chromosome is activated, an L or M cone is expressed with a probability n_L or n_M, respectively, as in a noncarrier normal trichromat, and when the abnormal, deutan, or protan X chromosome is activated, the gene expressed is always for an L or M cone, respectively. The modified n'_L is then the overall probability that an L cone gene is expressed. Hence, for the protan carrier, this probability is

$$n'_L(\text{protan carrier}) = p \cdot n_L, \tag{30}$$

because an L cone only occurs when the normal X chromosome is activated and, further, an L gene is chosen for expression. Similarly, for the deutan carrier (note that $n_L + n_M = 1$),

$$n'_L(\text{deutancarrier}) = p \cdot n_L + (1 - p) \tag{31}$$

$$= 1 - p \cdot n_M. \tag{32}$$

In Eq. (31), the first term $p \cdot n_L$ after the equal sign is the same as before, and the second term $(1 - p)$ is the probability that the abnormal X chromosome (which can only express an L cone) is activated. Hence, relative to noncarrier normal trichromats, the fraction of L cones is, on average, reduced in protan carriers and increased for deutan carriers. In either case, the distribution of L:M cone ratios deviates from that of the noncarrier normal trichromats. In particular, a small p value can lead to small n'_L for protan carriers [24] and large n'_L for deutan carriers. The chance for p much smaller than $1/2$ is quite substantial because the activated X chromosome in each cell is inherited from a small pool of (around seven or eight) precursor cells early in female embryological development [25]. Because our model predicts that extreme L-cone fractions lead to larger $f_{\text{matching-range}}$ values, female carriers of dichromacy should have, on average, a larger $f_{\text{matching-range}}$ value. This may explain the observation that such carriers have, on average, an $f_{\text{matching-range}}$ that is about two to three times that for noncarrier normal trichromats [19], though this difference in $f_{\text{matching-range}}$ has not been observed in other studies [26]. Regardless, our analysis above also leads to prediction 3: that a larger $f_{\text{matching-range}}$ is more likely to occur in a deutan than a protan carrier. This is because, typically, $n_L > n_M$ in normal noncarriers; hence, given each p value,

$$n'_L(\text{protan carrier}) = pn_L > 1 - n'_L(\text{deutan carrier}) = pn_M. \tag{33}$$

This means that the distance of n'_L(protan carrier) from the extreme 0 is larger than the distance of n'_L(deutan carrier) from the extreme 1, i.e., extreme L-cone fractions are more likely in deutan than protan carriers. Predictions 2 and 3 regarding the $f_{\text{matching-range}}$ in female carriers must be tested using sufficiently large (larger than those from the observations so far [19,26]) pools of female carriers for whom the spectral sensitivity of their underlying pigments is known and for whom the L:M cone ratio is known. New imaging techniques may allow for L:M ratio to be estimated more expeditiously in these subjects [27].

Now we come to prediction 4 on the strong tetrachromats. Both analytically and intuitively, when the fourth, abnormal, cone in the tetrachromats is more like one of the normal cones in terms of its sensitivities to the three lights, it is more likely for such a tetrachromat to find a match because such a tetrachromat is more like a normal trichromat. We should also consider the possibility of (female) tetrachromats who carry two different versions of abnormal L or M cones. For example, consider an individual with normal L cones but two different versions of the abnormal M cones. This individual would appear like a deuteranomalous who requires more green light than normal to match; however, she would be likely to have a smaller matching range than that of a typical (trichromatic) deuteranomalous.

Only females can be (strong) tetrachromats or normal trichromats who are also carriers of dichromacy. In the former case, our model predicts that their matching range should be smaller; in the latter case, their matching range is predicted to be likely larger. Hence, between males and females who are not color vision deficient, i.e., not dichromats or anomalous trichromats, there may or may not be a significant difference between the two genders in terms of the average matching range. Interestingly, Rodriguez-Carmona *et al.* [28] observed a larger matching range in a sample of females believed to be absent of any carriers of color vision deficiency. However, no genetic testing was performed in that study, and the statistical method of "removing" carriers from their sample is not ideal. To obtain clean data, it is best to test each prediction using only the corresponding group of females without contamination from the other group. Furthermore, it has been noted that most heterozygous females who are carriers of anomalous trichromacy are not strong tetrachromats who have their 4D color space preserved at the post-receptor level [19,20,29]. It is, thus, important to exclude the weak tetrachromatic subjects when testing the prediction about the tetrachromats because these weak tetrachromatics could have complex color matching behavior caused by their likely extra color dimension at the receptor, but not post-receptor, level [30]. Our formulation of the Rayleigh matching applies only when the dimensions of color information at the receptor level are preserved post-receptorally. Tests of various predictions of our modeling will help shed light on the mechanisms by which color signals are processed by the human visual system.

Funding. Gatsby Charitable Foundation; National Eye Institute (NEI) (R01EY017607, P30EY001931).

Acknowledgment. The research reported in this publication was supported (to L. Zhaoping) by the Gatsby Charitable Foundation and (to J. Carroll) by the National Eye Institute of the National Institutes of Health under award numbers P30EY001931 and R01EY017607. The content is solely the responsibility of the authors and does not necessarily represent the official views of the funders. We are grateful for the helpful comments by John L. Barbur.

REFERENCES

1. L. Rayleigh, "Experiments on colour," Nature **25**, 64–66 (1881).
2. W. A. Nagel, "I. Zwei Apparate für die augenärztliche Funktionsprüfung," Ophthalmologica **17**, 201–222 (1907).

3. L. T. Sharpe, A. Stockman, H. Jägle, and J. Nathans, "Opsin genes, cone photopigments, color vision, and color blindness," in *Color Vision: from Genes to Perception*, K. R. Gegenfurtner and L. T. Sharpe, eds. (Cambridge University, 1999), pp. 3–52.
4. J. Neitz and G. H. Jacobs, "Polymorphism of the long-wavelength cone in normal human colour vision," Nature **323**, 623–625 (1986).
5. J. Pokorny, V. C. Smith, and I. Katz, "Derivation of the photopigment absorption spectra in anomalous trichromats," J. Opt. Soc. Am. **63**, 232–237 (1973).
6. J. C. He and S. K. Shevell, "Variation in color matching and discrimination among deuteranomalous trichromats: Theoretical implications of small differences in photopigments," Vis. Res. **35**, 2579–2588 (1995).
7. P. Thomas and J. Mollon, "Modelling the Rayleigh match," Visual Neurosci. **21**, 477–482 (2004).
8. J. Barbur, M. Rodriguez-Carmona, J. Harlow, K. Mancuso, J. Neitz, and M. Neitz, "A study of unusual Rayleigh matches in deutan deficiency," Visual Neurosci. **25**, 507–516 (2008).
9. T. Lamb, "Photoreceptor spectral sensitivities: common shape in the long-wavelength region," Vis. Res. **35**, 3083–3091 (1995).
10. A. Stockman and L. T. Sharpe, "The spectral sensitivities of the middle-and long-wavelength-sensitive cones derived from measurements in observers of known genotype," Vis. Res. **40**, 1711–1737 (2000).
11. P. Lillywhite and S. Laughlin, "Transducer noise in a photoreceptor," Nature **277**, 569–572 (1979).
12. H. Barlow, "Retinal and central factors in human vision limited by noise," in *Vertebrate Photoreception*, H. Barlow and P. Fatt, eds. (Academic, 1977), pp. 337–358.
13. L. Zhaoping, W. Geisler, and K. May, "Human wavelength discrimination of monochromatic light explained by optimal wavelength decoding of light of unknown intensity," PLoS One **6**, e19248 (2011).
14. L. Zhaoping, *Understanding Vision: Theory, Models, and Data* (Oxford University, 2014).
15. J. Birch, "Classification of anomalous trichromatism with the Nagel anomaloscope," in *Colour Vision Deficiencies XI ocumenta Ophthalmologica Proceedings Series*, Springer 1993), pp. 19–24.
16. M. Neitz, J. Carroll, A. Renner, H. Knau, J. S. Werner, and J. Neitz, "Variety of genotypes in males diagnosed as dichromatic on a conventional clinical anomaloscope," Visual Neurosci. **21**, 205–216 (2004).
17. J. Barbur and M. Rodriguez-Carmona, "Variability in normal and defective colour vision: Consequences for occupational environments," in *Colour Design*, J. Best, ed. (Woodhead Publishing Limited, 2012), pp. 24–82.
18. R. C. Baraas, D. H. Foster, K. Amano, and S. M. Nascimento, "Color constancy of red-green dichromats and anomalous trichromats," Invest. Ophthalmol. Visual Sci. **51**, 2286–2293 (2010).
19. G. Jordan and J. Mollon, "A study of women heterozygous for colour deficiencies," Vis. Res. **33**, 1495–1508 (1993).
20. A. L. Nagy, D. I. MacLeod, N. E. Heyneman, and A. Eisner, "Four cone pigments in women heterozygous for color deficiency," J. Opt. Soc. Am. **71**, 719–722 (1981).
21. G. H. Jacobs and J. Neitz, "Electrophysiological estimates of individual variation in the L/M cone ratio," in *Colour Vision Deficiencies XI* (Springer, 1993), pp. 107–112.
22. J. Carroll, J. Neitz, and M. Neitz, "Estimates of L:M cone ratio from ERG flicker photometry and genetics," J. Vision **2**(8), 531–542 (2002).
23. M. F. Lyon, "Gene action in the X-chromosome of the mouse (Mus musculus L.)," Nature **190**, 372–373 (1961).
24. E. Miyahara, J. Pokorny, V. C. Smith, R. Baron, and E. Baron, "Color vision in two observers with highly biased LWS/MWS cone ratios," Vis. Res. **38**, 601–612 (1998).
25. G. H. Jacobs and G. A. Williams, "L and M cone proportions in polymorphic new world monkeys," Visual Neurosci. **23**, 365–370 (2006).
26. E. Konstantakopoulou, M. Rodriguez-Carmona, and J. L. Barbur, "Processing of color signals in female carriers of color vision deficiency," J. Vision **12**(2):1–11 (2012).
27. R. Sabesan, H. Hofer, and A. Roorda, "Characterizing the human cone photoreceptor mosaic via dynamic photopigment densitometry," PloS One **10**, e0144891 (2015).
28. M. Rodriguez-Carmona, L. Sharpe, J. Harlow, and J. Barbur, "Sex-related differences in chromatic sensitivity," Visual Neurosci. **25**, 433–440 (2008).
29. G. Jordan, S. S. Deeb, J. M. Bosten, and J. Mollon, "The dimensionality of color vision in carriers of anomalous trichromacy," J. Vision **10** (8):1–19 (2010).
30. Y. Sun and S. K. Shevell, "Rayleigh matches in carriers of inherited color vision defects: The contribution from the third L/M photopigment," Visual Neurosci. **25**, 455–462 (2008).